Design tradeoffs for a high spectral resolution mid-infrared echelle spectrograph on the Thirty-Meter Telescope

A.T.Tokunaga[a*], T. Bond[a], J. Elias[b], M. Chun[a], M. Richter[c], M. Liang[b], J. Lacy[d], L. Daggert[b], E.Tollestrup[a], M.Ressler[e], D. Warren[f], S. Fisher[g], J. Carr[h]

[a]Institute for Astronomy, Univ. of Hawaii, 2680 Woodlawn Dr., Honolulu, HI 96822
[b]National Optical Astronomy Observatories, 950 N. Cherry Ave, Tucson, AZ 85719
[c]University of California, 1 Shields Ave, Davis, CA 95616
[d]University of Texas, 1 University Station- C1400, Austin, TX 78712
[e]Jet Propulsion Lab, 4800 Oak Grove Dr., Pasadena, CA 91109
[f]David Warren Optical Design Services, Los Angeles, CA 90035
[g]Gemini Observatory, 670 N. A'ohoku Place, Hilo, HI 96720
[h]Naval Research Lab, Remote Sensing Div., Washington, DC 20375

ABSTRACT

A feasibility design study was undertaken to assess the requirements of a mid-infrared echelle spectrograph (MIRES) with a resolving power of 120,000 and its associated mid-infrared adaptive optics (MIRAO) system on the Thirty-Meter Telescope. Our baseline design incorporates a 2Kx2K Si:As array or array mosaic for the spectrograph and a 1Kx1K Si:As array for the slit viewer. Various tradeoffs were studied to minimize risk and to optimize the sensitivity of the instrument. Major challenges are to integrate the spectrograph to the MIRAO system and, later, to an adaptive secondary, the procurement of a suitable window and large KRS-5 lenses, and the acquisition of large format mid-IR detector arrays suitable for the range of background conditions. We conclude that the overall risk is relatively low and there is no technical reason that should prevent this instrument from being ready for use at first light on the Thirty-Meter Telescope.

Keywords: infrared, spectroscopy, imaging, echelon, echelle, Thirty-Meter Telescope

1. INTRODUCTION

Planning has started for the design of the Thirty-Meter Telescope (TMT) and its instrument complement[1,2]. One of the instruments being considered is the Mid-Infrared Echelle Spectrograph (MIRES). The detailed scientific rational and requirements of MIRES are discussed elsewhere at this meeting[3]. MIRES will provide a tremendous leap in sensitivity and speed for high-resolution spectroscopy and high-spatial resolution imaging in the thermal infrared (5-25 μm). These gains translate into the opportunity to address some of the most compelling problems of our time: the origin of planetary systems and the origin of life on Earth. By the time TMT sees first light (~2015 at the earliest), considerable resources will have been spent searching for and characterizing extrasolar planetary systems with the Kepler mission, Space Interferometry Mission, Gemini Precision Radial Velocity Spectrometer, Gemini Planet Imager, Atacama Large Millimeter Array, and the James Webb Space Telescope).

* Further author information: Send correspondence to A.T. Tokunaga.
Email: tokunaga@ifa.hawaii.edu, telephone: 808-956-6691.

Ground-based and Airborne Instrumentation for Astronomy, edited by Ian S. McLean, Masanori Iye,
Proc. of SPIE Vol. 6269, 62693Y, (2006) · 0277-786X/06/$15 · doi: 10.1117/12.670169

In view of the rich set of observational capabilities that are expected to be available in the time period beyond 2015. we have identified a set of scientific programs that can be *uniquely* carried out with the TMT. This has driven the scientific requirements to very high spectral resolution ($R=\lambda/\Delta\lambda=120{,}000$) in the mid-infrared. At this resolving power MIRES would have unmatched sensitivity and angular resolution for the study of molecular emission and absorption features. MIRES also has a slit-viewer that will allow high-angular resolution imaging to be accomplished. MIRES on the TMT will be a powerful tool for probing planet formation environments for clues to the physical origin of planetary architectures (planetary masses, orbital radii, and eccentricities). These clues will be critical in developing a theory of planet formation that can predict outcomes under a broader range of initial conditions than can be directly observed. While ALMA and JWST will study the outer regions of planet-forming disks, MIRES will provide a direct look at the inner disk regions where terrestrial and giant planets form.

In order to obtain the best possible image quality and throughput with MIRES it is necessary to utilize a laser guide star system. Known as the Mid-Infrared Adaptive Optics (MIRAO) system, it is described elsewhere at this meeting[4]. The design of MIRAO and MIRES was done in a unified way with a single team involved in both instruments. This has led to a comprehensive, fully self-consistent end-to-end design.

We present in this paper a description of the major design tradeoffs for MIRES that were developed as part of our feasibility study of MIRES. This should be considered a work in progress. We have not completed a conceptual design study, and therefore many of the choices to be made are still under study. In our work to date, every effort was made to ensure that MIRES will be cost-effective. Thus the instrumental requirements and design are aimed at only the unique science that can be accomplished with MIRES and not at all of the science that such an instrument could potentially do. For example, we did not consider scientific objectives that would be pursued by the Mid-Infrared Instrument on JWST.

2. OPTICAL DESIGN

2.1. Scientific requirements.

MIRES consists of two major components, the high-resolution spectrograph and the slit-viewing camera. The latter can also operate as a stand-alone camera for imaging at 4.5-25 μm. Table 1 summarizes the basic instrument requirements. The schematic of the optical path is shown in Figure 1. In this schematic the refractive optical design is shown. An alternative all-reflecting design is discussed in Section 4.4.

Table 1. Basic instrument characteristics.

Mode	Diffraction-limited
Wavelength range	4.5-25 μm
Spectrograph	
Slit length	3"
Slit width	≥ 0.1" (R ≤ 120,000)
Spectral resolving power	60,000-120,000
Echelon	82.9° blaze angle, 0.50 lines/mm ruling
Spectrograph pixel scale	0.024 "/pixel at 4.5-14 μm; 0.038 "/pixel at 17-25 μm
Spectrograph focal plane	2Kx2K Si:As array
Emissivity	Estimated to be 9% for the telescope primary and secondary; 4% for MIRAO relay optics; 1% for MIRAO without relay optics
Slit-viewing camera	
Field of view	15"x15"
Camera pixel scale	0.015 "/pixel
Camera focal plane	1Kx1K Si:As array
Nodding	Required
Chopping	Not required

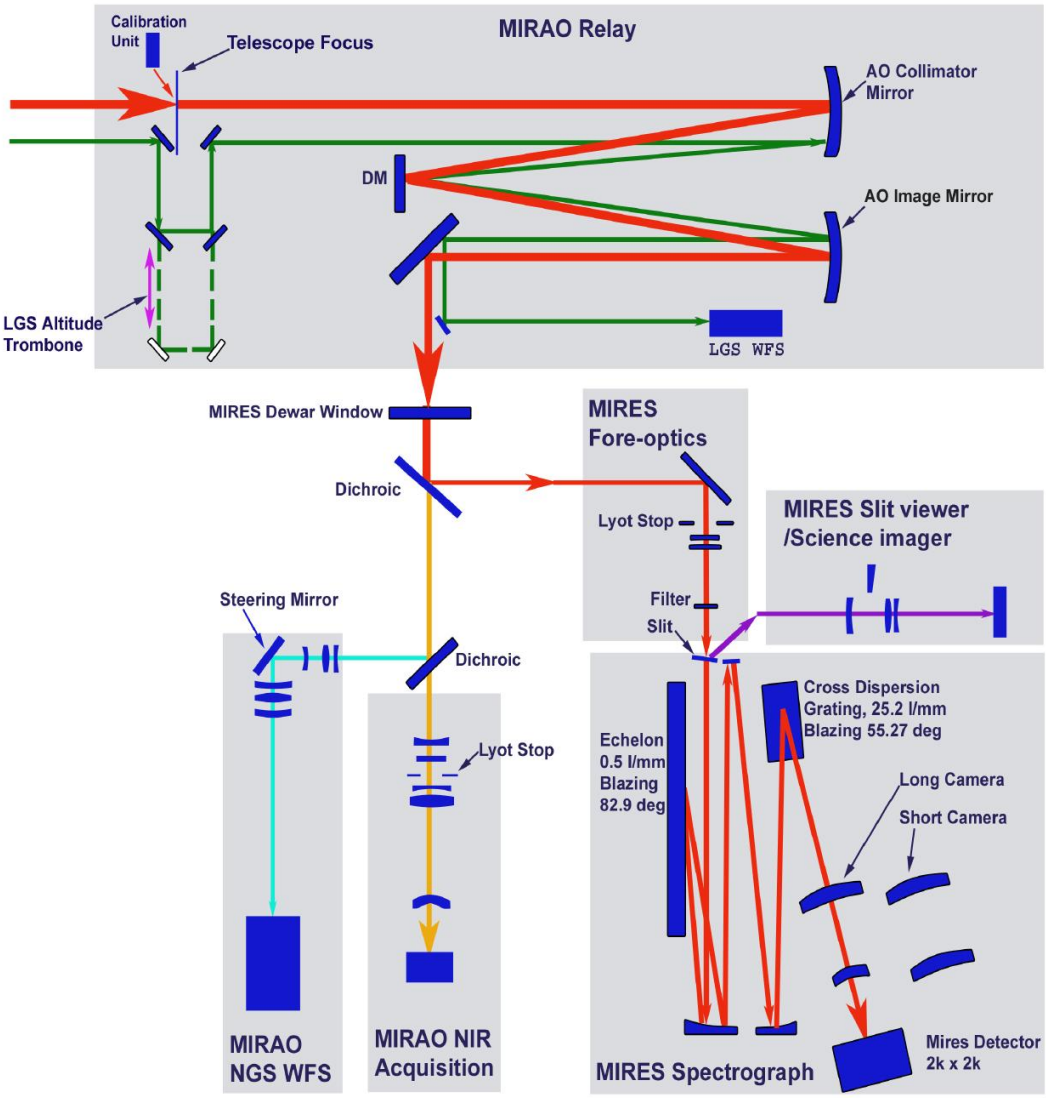

Figure 1. Schematic of the MIRAO/MIRES optical path. The MIRES cryostat encompasses the MIRES fore-optics, slit viewer/science imager, spectrograph, MIRAO natural guide star sensor, and the MIRAO near-infrared acquisition camera. The only warm optical element in the MIRES section of the instrument is the cryostat entrance window. The MIRAO design is discussed by Chun et al.[4] and the integrated optical design of MIRAO/MIRES is discussed by Liang et al.[5]

The telescope focus is situated in front of the MIRES cryostat window. After the beam passes through the window the 4.5-25 μm light is reflected off a dichroic to the spectrographic channel. The transmitted light is sent to one of 3 wave-front sensors (WFSs). From the dichroic, the light goes to an image rotator if it is decided to keep the instrument stationary. Alternatively, MIRES could be rotated and the image rotator would be removed from the optical train. There is a pupil image before the slit, and the slits are in a wheel for slit selection. The reflected light is sent to the slit viewing camera which also doubles as a science camera. Thus the slit wheel will contain a flat mirror for imaging. The slit-viewing camera also has a filter wheel with 15 filter positions.

The light passing through the slit goes to the spectrograph. An order sorting filter wheel is located directly after the slit. An off-axis parabola collimates the light and sends it to the echelon. The dispersed light from the echelon returns to the off-axis parabola and is imaged on a powered mirror. The light then goes to a second off-axis parabola which collimates the light and sends it to a cross-disperser. After the cross-disperser there are two cameras, one for short wavelengths (<14 μm) and one for long wavelengths (>17 μm). The design approach for the spectrograph section follows that of the TEXES instrument[6] that has been successfully used at the NASA Infrared Telescope Facility and Gemini-North.

3. OPTO-MECHANICAL LAYOUT

An opto-mechanical layout of the MIRAO/MIRES is shown in Fig. 2. Three major goals were pursued while developing the instrument layout: (1) To be able to feed a second instrument from the MIRAO module. (2) To be able to use MIRES in either a horizontal or a vertical orientation. This allows a tradeoff study between an internal image rotating mechanism vs. rotating the entire instrument. This trade study is contemplated for the conceptual design. (3) To be able to accommodate a future TMT upgrade to an adaptive secondary mirror by simply removing the MIRAO relay and retaining the remaining optics. All three goals were achieved in the adopted design concept.

3.1. MIRES slit-viewing/science camera

The mid-infrared slit-viewing camera has a 15"x15" field of view; see Figure 2. A rotating cold stop, 58 mm in diameter, is located at the pupil image located between the cryostat window and the slit, and it masks the secondary and its support structure. The camera lenses image the focal plane onto the detector array, which is mounted on a focus stage. There is a pupil located between the lenses and the detector, and a 15-position filter wheel located here. The filters are 15 mm in diameter and the filter wheel is 130 mm in diameter. The volume representing the detector package and focus stage is 150 mm x 150 mm x 300 mm.

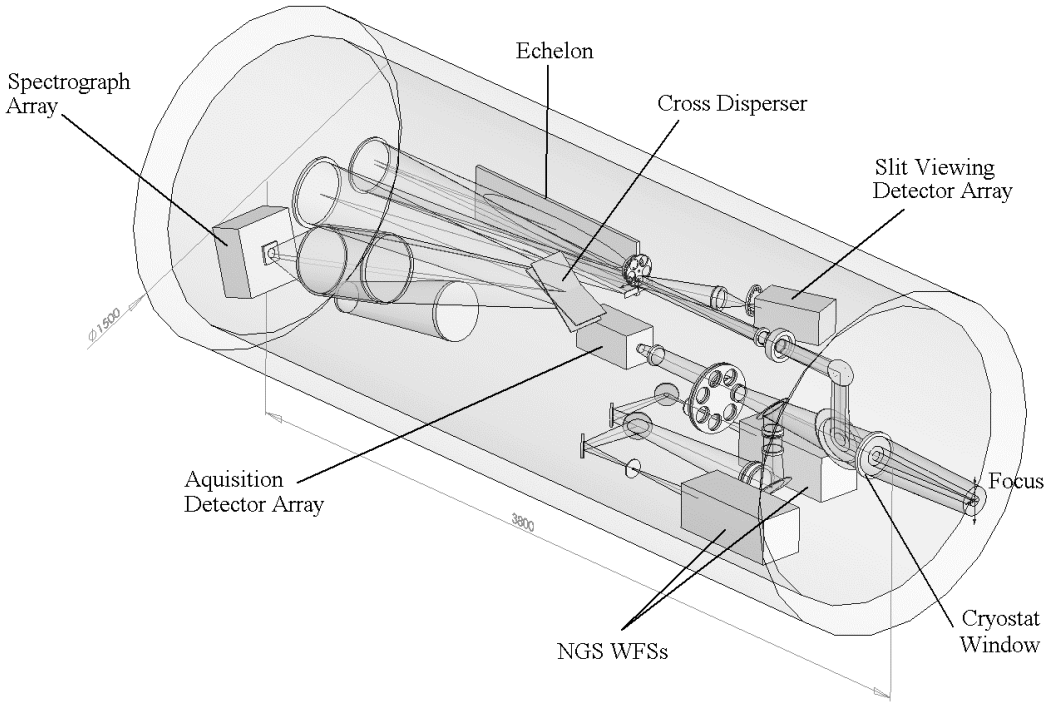

Figure 2. Instrument opto-mechanical layout. The cryostat has a diameter of 1.5 m and a length of 3.8 m.

3.2. MIRES spectrograph

The slit wheel mechanism has 5 positions (4 slits and a mirror for imaging); see Figure 3. Immediately behind the slit is a filter wheel with 12 positions. The outer diameter of the slit wheel is 140 mm and the outer diameter of the filter wheel is 110 mm. Off-axis parabola (OAP) #1, OAP #2, the echelon, and the powered fold mirror are all fixed optical components. OAP #1 has an outer diameter of 240 mm and OAP #2 has an outer diameter of 300 mm. The single cross disperser requires a mechanism in order to tilt it over a range of about 30°. There is no requirement for a second cross disperser grating.

The spectrograph has been designed to accommodate two pixel scales, and therefore it incorporates a turret containing a long focal length camera and a short focal length camera. A mechanism will be required for switching between these two camera optics, and the mechanical layout has space allocated for this mechanism. We also require a mechanism to provide focus and a small range of tilt of approximately 3° to provide good optical quality with the two cameras. A volume that is 300 mm x 300 mm x 150 mm is shown for this mechanism as well as the detector head.

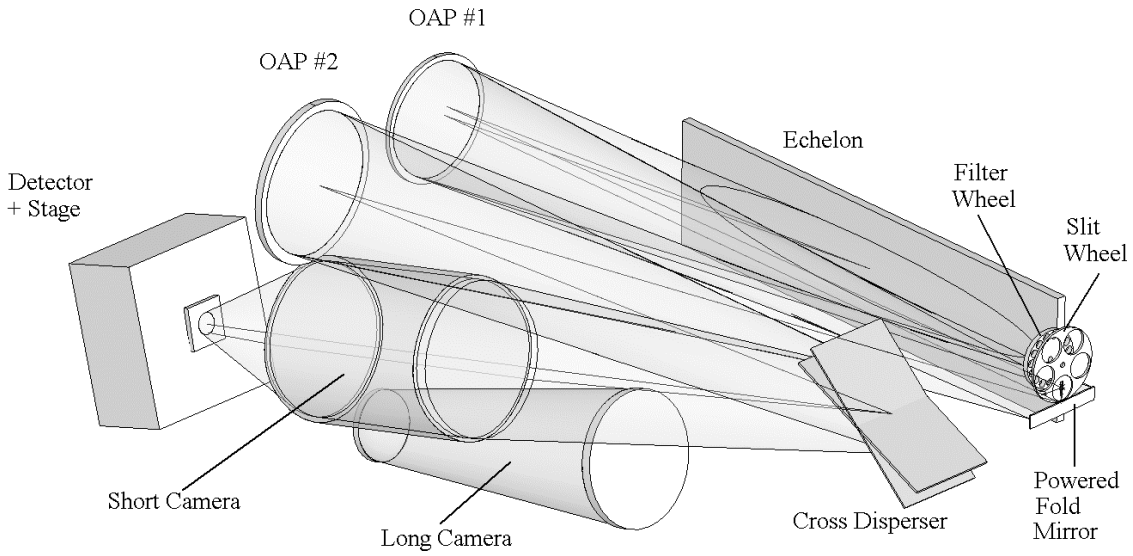

Figure 3. Spectrograph layout. See Fig. 1 for a schematic of the optical path. The short camera is in the light path while the long camera is shown in the stowed position. The echelon is fixed, but the cross-disperser has variable tilt mechanism.

4. TRADEOFFS

4.1. Instrument rotation tradeoff issues

A mechanical layout of MIRES combined with MIRAO is shown in Figure 4. The floor is nominally located 2 m below the focal plane of the telescope. This configuration would require an internal K-mirror for image derotation, so that the spectrograph is not subject to a varying gravity vector. The benefits of mounting in this orientation include the elimination of cable wraps for all services, the ease of access to all sections of the instrument, and stiff mounting surfaces available for installation. However, this configuration has the largest footprint on the Nasmyth platform. A very rough estimate of the mass of the instruments shown in Figure 4 is 3 metric tons for MIRES and 2 metric tons for MIRAO.

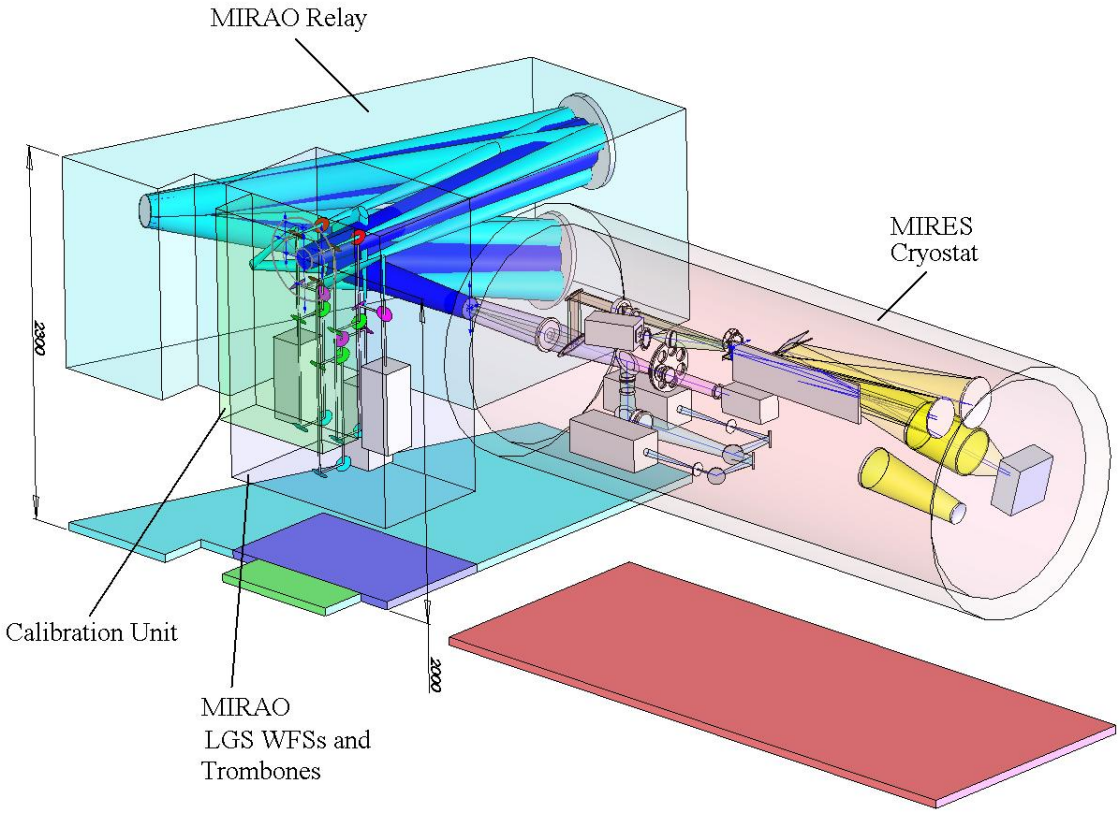

Figure 4. MIRAO/MIRES combined opto-mechanical layout. The beam from the telescope is 2 m above the Nasmyth floor, and the footprint on the floor is shown.

Figure 5 shows the MIRAO relay removed for use with an adaptive secondary. The advantages of this configuration are similar to those for the configuration in Figure 4, but with the very significant added benefit that MIRES is fed directly from the telescope without any warm fold mirrors in the science path. This is the configuration that provides the lowest emissivity and the highest sensitivity.

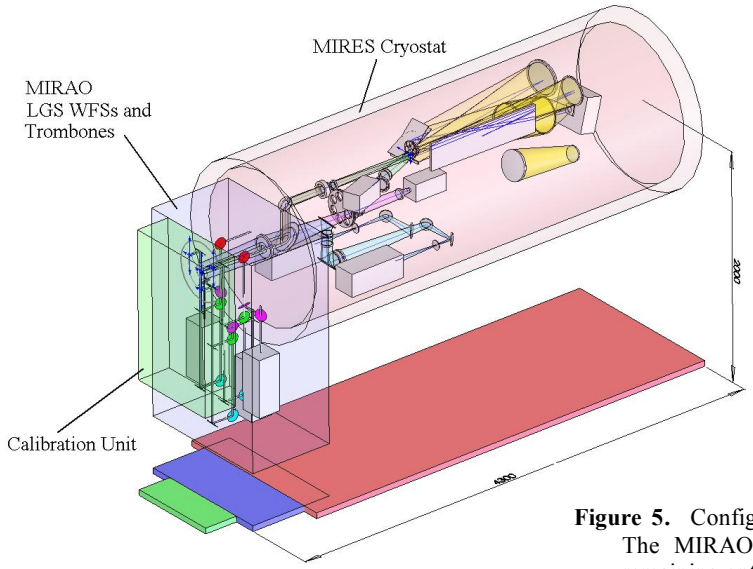

Figure 6 illustrates the configuration with the instrument oriented vertically. In this configuration, the entire instrument is rotated to match the image rotation. Since the instrument is vertical, it does not have any variation in flexure in the direction of gravity. The floor is shown 2 m

Figure 5. Configuration for use with an adaptive secondary. The MIRAO relay optics have been removed but the remaining optics can be used without modification.

below the science focus, and the instrument protrudes below the Nasmyth floor. Note that MIRES could be rotated 180° so that the instrument is downward looking. In either case, access is more difficult than in the horizontal configuration, but the footprint on the platform is smaller.

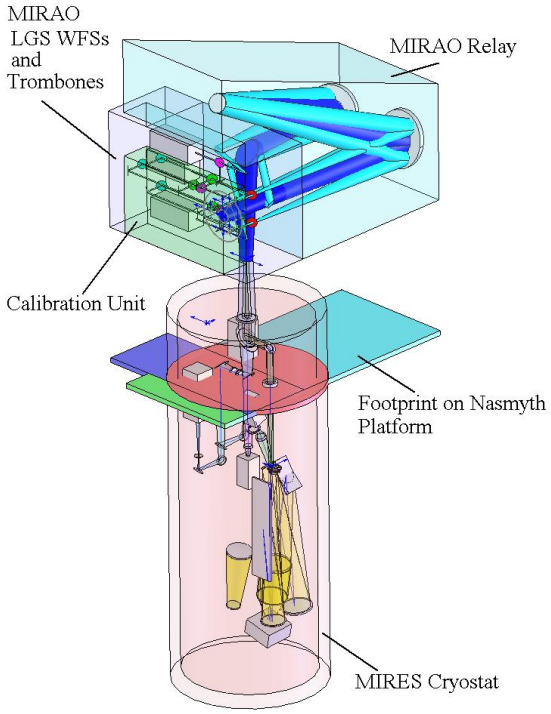

Figure 6. Vertical orientation of MIRAO/MIRES.

4.2. Window requirements

The spectrograph requires coverage from 4.5-5 μm and the wave-front sensors inside of the cryostat requires coverage from 1-2.5 μm. Thus the large 1-25 μm wavelength range that the window must accommodate presents two major problems for the selection of the window material. First, the window must have high transmission across this wavelength range and there are few viable material choices. Hygroscopic materials such as KBr and CsI are often used as windows in mid-IR instruments, but for a large complex instrument like MIRES the prospect of frequent changes of the window is a major disadvantage. A non-hygroscopic material with the appropriate wavelength coverage is KRS-5, but it has high reflective losses. This can be minimized with anti-reflection coatings, although covering the entire 1-25 μm spectral range with a high transmission anti-reflection coating is infeasible. Since the window is large (200 mm diameter), KRS-5 also has potential problems with meeting the required homogeneity requirements and there is only a limited number of vendors who could supply this material. There is some doubt that the current vendors will be able to fabricate this material in the future due to environmental restrictions. A possible solution is to utilize a large ferro-fluidic seal that would permit the use of multiple windows or to use a vacuum gate valve that allows changing of the window without bringing the entire instrument to atmospheric pressure.

Second, the emissivity of the window must be kept to a minimum. Ideally, we would like the emissivity of the window to be no higher than 2%. This requires high performance anti-reflection coatings. Therefore it would be best to have one window optimized for 4.5-5 μm, one for 8-14 μm, and one for 17-25 μm. This would favor a mechanism using a ferro-fluidic seal that would allow different windows to be used. While a detailed study of the tradeoffs has not been made, there are solutions to meeting the requirements of providing a low-emissivity window.

4.3. Array, Pixel, Slit and Camera Trades

There are several trades involving the spectrograph array size, slit length, pixel scale, and camera design. These are best considered together. We took as a starting point that the instrument should be optimized for the 7-14 μm region (the "10-μm window"). For the 5 μm region the array will be significantly under-filled and will also have a more limited slit length, but since this mode of the instrument should eventually be replaced by a 3-5 μm spectrograph, this was an acceptable compromise.

For the 18-25 μm region the problem is that the spectra are no longer contiguous orders. If only a single feature is to be observed, this is not much of a problem. However, if there are multiple lines to be observed, and they cannot fit on the array in a single configuration, the observing time doubles. Furthermore, one cannot use a single stable setting for the observation; instead one must adjust grating tilt and calibration and sky removal will be limited by mechanical repeatability.

Another consideration is the slit length. Although it could be argued that a slit only a few times longer than the diffraction core width would be enough, there can be significant power in the image halo, and there are a number of

programs where objects are extended on modest spatial scales. We therefore settled on a slit length of 3". We adopted a scale of 0.024"/pixel, while retaining the requirement that the instrument provide R=100,000 at 10 μm with a 0.1" slit. This allows full sampling of the diffraction core at 14 μm and reasonable sampling at 5 μm.

These design choices severely limit spectral coverage if a 1Kx1K array is used. The spectral coverage with a 2Kx2K format within the 7-14 μm region ranges from just over 2% to just under 4%; the coverage using a 1Kx1K array would be 4 times less, or less than one percent bandwidth for all wavelengths. Our science case requires coverage of 2% or more for many programs, so that a smaller array would in many cases lead to a factor of 4 increase in observing time, relative to the 2Kx2K mosaic. For the 20-μm window continuous spectral coverage can be provided out to 25 μm (the effective useful limit of atmospheric transmission) using the same echelon grating but a coarser pixel scale of 0.038"/pixel.

The desire for more than one pixel scale leads naturally to a choice of refractive optics. In a future conceptual design study, the feasibility of using refractive optics will be investigated in more detail. If this is deemed too risky due to problems with using KRS-5, an all-reflective design with a single pixel scale is acceptable (see Section 4.4) but it would provide non-contiguous spectra over part of the 20-μm region.

4.4. Reflective vs. refractive optics for the spectrograph

The choice of using refractive optics for the spectrograph was driven by the desire to have two pixel scales, one optimized for 14 μm and another for 20 μm. This will provide optimum sampling of the spectral lines. However this design uses KRS-5 lenses. As the largest lenses are 300 mm in diameter and we are not certain about the quality and availability of KRS-5 in the future, we may choose to switch to an all-reflecting design at the conceptual design stage. Indeed an all-reflecting design was accomplished for the proposal for this feasibility study. The approach was to use a three-mirror anastigmatic for the collimator and the camera optics. This design is shown in Figure 7.

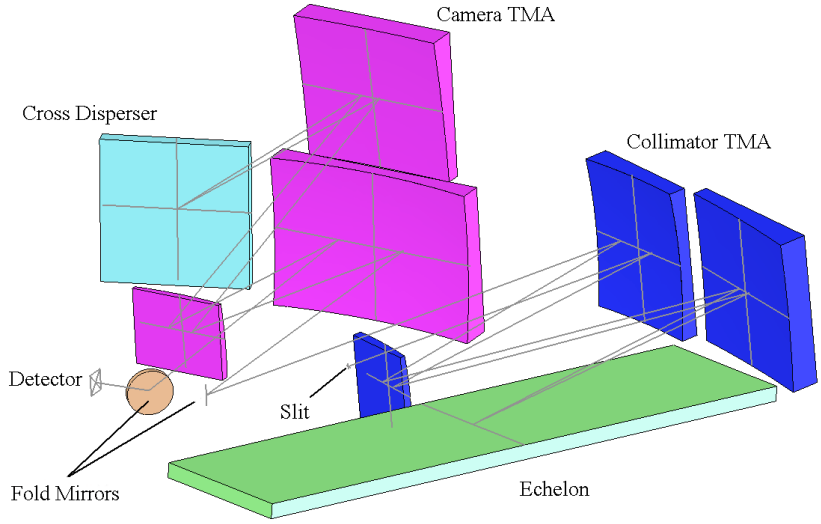

The main disadvantage of this design is that we can accommodate only one pixel scale for the spectrograph. Given the choice of only pixel scale, we would optimize it for 14 μm. This would allow good sampling for 8-14 μm but with some under-sampling of the diffraction-limited core at 4.5-5 μm and over-sampling at 17-25 μm. Nonetheless, the experience of the TEXES observations has been that this is a good compromise for most observations.

Figure 7. A design utilizing an all-reflecting optics for the spectrograph. Although space does not allow a full discussion of this design, we were able to meet our image quality requirements using a 2Kx2K array.

4.5. Slit diffraction effects

Because the dimensions of the slit are comparable to the diffraction-limited point spread function (PSF) at the infrared operating wavelengths of MIRES, the throughput, spectral resolution, and signal/noise calculations must account for diffraction at the slit as well as vignetting of the diffracted energy by the spectrograph optics. These effects were modeled using a physical optics analysis code (PHOCAS) developed by Dr. Richard Boucher (private communication) to account for the partially coherent nature of the image at the slit and subsequent propagation through the spectrograph. Figure 8 shows how PHOCAS models the spectrograph system. The spectrograph is treated only as a black box with an f/ratio and perfect imaging between slit and focal plane.

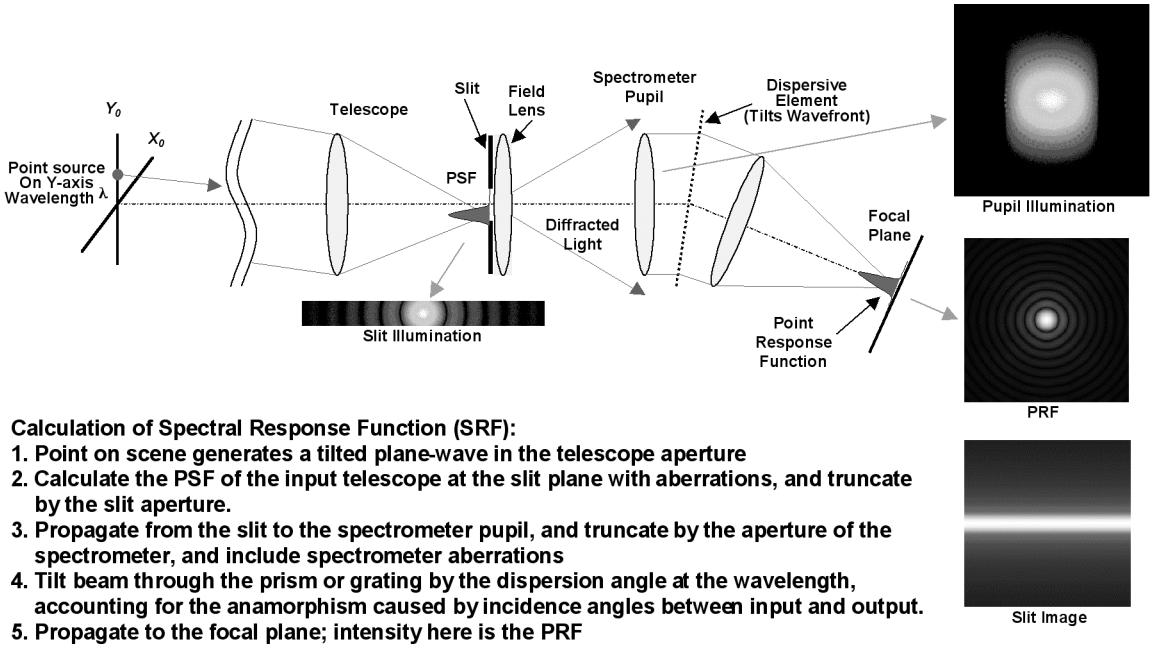

Figure 8. Schematic PHOCAS model of the spectrograph light path.

Figure 9 shows the image of a monochromatic point source at the focal plane for two different slit widths. The nominal slit width, 200 μm, corresponds to about 0.09" at the f/15 telescope focus. There is considerable truncation of the energy in the telescope point spread function (PSF) by the slit as well as vignetting of the energy that is diffracted out of the geometric light path. Widening the slit increases the overall energy in the image without significantly broadening its width. Figure 10 illustrates the benefits of oversizing the spectrograph optics to capture more of the energy diffracted at the slit. The overall intensity of the spectrograph image increases and its width decreases.

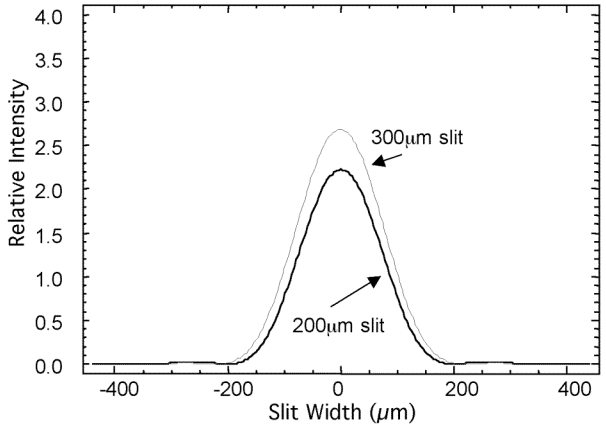

Figure 9. Image of a monochromatic (10 μm) point source at the spectrograph focal plane: f/15 telescope image, 200 and 300 μm slits, f/15 spectrograph optics.

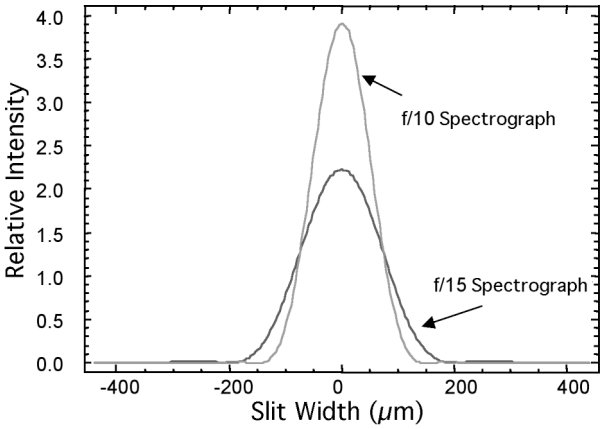

Figure 10. Image of a monochromatic (10 μm) point source at the spectrograph focal plane: f/15 telescope image, 200 μm slit and f/15 and f/10 spectrograph optics.

Widening the slit increases the throughput of the spectrograph but also increases the background reaching the focal plane. Thus we use the following figure of merit for the signal-to-noise in the background-limited case: point source signal/(background signal)$^{0.5}$. This parameter is shown in Table 2 for a point source and indicates a fairly broad optimum signal-to-noise around a 200 μm slit and f/12.5 to f/10 spectrograph optics. Interestingly, it shows that it is possible to go too far in oversizing the spectrograph such that background is captured preferentially over signal and signal-to-noise is reduced.

Table 2. Signal-to-noise ratio for a point source as a function of slit width and spectrograph focal ratio.

	Signal/(Background)$^{0.5}$			
slit width (μm)	**f/15**	f/12.5	f/10	f/7.5
100	0.468	0.577	0.693	0.804
120	0.611	0.737	0.855	0.939
140	0.744	0.876	0.981	1.025
160	0.858	0.930	1.063	1.067
180	0.945	1.053	1.099	1.076
200	**1.000**	1.084	1.100	1.065
220	1.025	1.084	1.075	1.040
240	1.024	1.057	1.033	1.004
260	0.999	1.014	0.982	0.959
280	0.960	0.961	0.927	0.909
300	0.912	0.904	0.872	0.857

5. OTHER ISSUES

5.1. Echelon procurement

The fabrication of the echelon is a challenging item because of the high precision required on the groove spacing and the large size of the echelon. However the echelon we require for MIRES is similar in size to that fabricated for TEXES (863 mm x 110 mm for MIRES vs. 915 mm x 85 mm for TEXES)[6,7]. Thus while challenging to fabricate, the echelon is not a high risk item.

5.2. Detector requirements

We first consider the expected detected photon rates for the spectroscopic and imaging arrays. For the spectral minimum rate, we calculate the values assuming an adaptive secondary is present (9% system emissivity) and no atmospheric emission. The spectral maximum rate comes from observing a blackbody at ambient temperature, as might be done for spectral flat-field calibrations. For the imaging minimum, we consider 1% filters with an adaptive secondary and no atmospheric emission. The imaging maximum corresponds to observing a blackbody at ambient temperature with 10% bandpass. We choose these extreme cases because our goal is to be safely within detector performance margins. The detected photon rates are shown in Table 3 and illustrate why the spectral channel requires a low-flux detector while the imaging channel requires a high-flux detector.

Table 3. MIRES photon rates.

Wavelength [μm]	Photon Rate [detected photons/sec/pixel]			
	Spectroscopy		Imaging	
	Minimum	Maximum	Minimum	Maximum
5	60	660	1.20E+5	1.30E+7
8	1100	13000	2.20E+6	2.40E+8
10	2500	28000	4.90E+6	5.40E+8
12	3900	44000	7.60E+6	8.50E+8
18	9000	100000	1.20E+7	1.30E+9
20	8800	98000	1.10E+7	1.30E+9
22	8000	89000	1.00E+7	1.20E+9
24	6800	75000	8.80E+6	9.70E+8

The two most prominent detector array vendors for astronomical mid-infrared applications are Raytheon Vision Systems and DRS Infrared Sensors. Both companies have a long history of producing devices for ground-based instruments (MIRAC, MIRLIN, OSCIR, MICHELLE, etc.) and space-based observatories (Spitzer, WISE, JWST), and both are actively developing larger format high-flux arrays. However, it is uncertain whether the mid-infrared astronomical market will be able to support both vendors much beyond the current development efforts.

5.3. Coolers

The surface area of the MIRES dewar presented above is roughly 18 m^2. Reasonably conservative assumptions suggest a radiation load on the internal structure of ~120 W, with additional heat sources <30W. The cold mass was estimated to be 700 kg. The energy required to cool this from 300 K to 80 K is roughly $1x10^8$ J, and the energy required to cool from 80 K to 20 K is roughly $6x10^6$ J, assuming the bulk of the mass is aluminum.

Additionally, it is important to minimize vibrations introduced by the cooling system, which leads to a strong preference for pulse tube coolers, liquid cryogens, or external cooling loops. Pulse tube coolers have the additional advantage of greater reliability (longer service intervals) than Gifford-McMahon coolers, because they have fewer moving parts.

In our feasibility study we have adopted the following approach:

- Liquid nitrogen pre-cool.
- Two Cryomech PT 810 pulse tube coolers; the first stage of each is attached to radiation shielding ("active" shield) and the second stage to the optical bench.
- Two Cryomech PT 410 pulse tube coolers; the first stage of each is also attached to radiation shielding while the second stage is attached to one of the 10-μm science detectors.

The choice of Cryomech coolers is somewhat arbitrary at this time, and the market would be assessed in the conceptual design stage.

5.4. On sky chopping

Experience with TEXES, a high-resolution mid-IR spectrograph, has already demonstrated that spectroscopic observations can be carried out without sky chopping. Since spectroscopic targets would be relatively bright,

degradation of imaging performance without sky chopping would be tolerable for purposes of acquisition and guiding. But for imaging science, the potential degradation is a greater concern. We therefore carried out an investigation of performance of chopped vs. unchopped imaging observations, using MICHELLE on Gemini. This investigation indicated that the unchopped performance in a filter relatively unaffected by strong telluric features was within a factor of about 2 of the chopped performance. This estimate includes allowance for the greater on-target efficiency unchopped. This means that TMT, without chopping, would have sensitivity to point sources as good or better than a chopping, diffraction-limited 20-m telescope but with 1.5 times the spatial resolution when observing resolved objects. We do not yet understand the reason for the lower sensitivity without chopping. It could be due to sky noise, array readout noise or instability, or some combination. It may well be possible to reduce or eliminate the performance difference through a combination of improvements in observing procedures, detectors, and detector electronics. Further study to better understand the noise sources and identify possible improvements will be carried out as part of future MIRES studies.

ACKNOWLEDGMENT

The authors gratefully acknowledge the support of the TMT partner institutions. They are the Association of Canadian Universities for Research in Astronomy (ACURA), the Association of Universities for Research in Astronomy (AURA), the California Institute of Technology and the University of California. This work was supported, as well, by the Canada Foundation for Innovation, the Gordon and Betty Moore Foundation, the National Optical Astronomy Observatory, which is operated by AURA under cooperative agreement with the National Science Foundation, the Ontario Ministry of Research and Innovation, and the National Research Council of Canada.

REFERENCES

1. J. E. Nelson and G.H. Sanders, "TMT Status Report," *Proc. SPIE* 6267-60 (2006).
2. TMT web site: http://www.tmt.org/.
3. J. H. Elias, A. T. Tokunaga, M. J. Richter, J. S. Carr, M. R. Chun, M. C. Liu, J. H. Lacy, J. Najita, M. E. Ressler, S. E. Strom, M. Liang, and T. W. Bond, "Design of the TMT mid-infrared echelle: science drivers and design overview," *Proc. SPIE* 6269-141 (2006).
4. M. R. Chun, J. Elias, B. L. Ellerbroek, M. Liang, T. W. Bond, R. M Clare, A. T Tokunaga, M. Richter, and L. G. Daggert, "Design of the TMT mid-infrared adaptive optics system," *Proc. SPIE* 6272-26 (2006).
5. M. Liang, J.H. Elias, A.T. Tokunaga, M.R. Chun, and M.J. Richter, "Preliminary optical design for the TMT mid-infrared adaptive optics system and echelle spectrograph", *Proc. SPIE* 6269-150 (2006).
6. J. H. Lacy, M. J. Richter, T. K. Greathouse, D. T. Jaffe, and Q. Zhu, "TEXES: A Sensitive High-Resolution Grating Spectrograph for the Mid-Infrared," *Pub. Astron. Soc. Pacific* 114, 153-168 (2002).
7. B. Bach, K. Bach, B. W. Bach, and M. Schulze, "Modern echelons and echelles for infrared spectroscopy," *Proc. SPIE* 5901, 184 (2005).